Late-Transition-Metal Complexes with Bisazaferrocene Ligands for Ethylene Oligomerization

Eric V. Salo and Zhibin Guan*

Department of Chemistry, University of California, Irvine, California 92697-2025.

Received July 17, 2003

Herein we report the synthesis, characterization, and ethylene polymerization properties of novel C_2-symmetric and unsymmetric bisazaferrocene complexes with late-transition-metal Ni(II) and Pd(II). In the designed complexes, the two sp^2-hybridized nitrogen atoms in the azaferrocene rings coordinate to the transition metals with the azaferrocene architecture presenting pentamethyl or pentaphenyl cyclopentadiene (Cp* or Cp°) rings above and below the coordination plane for the purpose of preventing the associative chain transfer processes of ethylene from the axial faces. The Ni(II) and Pd(II) complexes were prepared and characterized by mass spectrometry (MS), ^{1}H and ^{13}C nuclear magnetic resonance (NMR) spectroscopy, elemental analysis, and single-crystal X-ray crystallography. Upon activation with methylaluminoxane (MAO), the bisazaferrocene complexes with $NiBr_2$ (**2a**) and $PdCl_2$ (**2b**) showed very low activities toward ethylene polymerization. Well-defined preactivated bisazaferrocene-Pd(II) complexes (**5** and **6**) exhibited relatively high thermal stability for ethylene oligomerization: *for example, complex* ***5*** *remains active in ethylene oligomerization at temperatures up to 120 °C.* They have moderate activities in ethylene polymerizations to form relatively low molecular weight oligomers. The polyethylene oligomers formed have branching densities ranging from 20 to 60 branches/1000 carbons. To overcome the difficulty encountered in the synthesis of complex **6**, a novel route was developed to make Pd(Me)Cl complexes with various dinitrogen ligands by in situ ligand substitution reaction. Finally, to gain mechanistic insight into the low reactivity of the bisazaferrocene-Pd^{II} complexes (**5** and **6**) as compared to their α-diimine counterparts, kinetic studies were undertaken to measure the energetic barriers for the first methyl migration and subsequent ethylene consumption. It was found that the insertion barriers ($\Delta G^{\ddagger}$) for both the first methyl migration and subsequent ethylene insertion for complex **5** were about 2−3 kcal/mol higher than the values for the α-diimine counterparts, which corresponds to a 2-order difference in the rate of polymerization. Variable-temperature experiments further revealed that the higher ethylene insertion barrier for the bisazaferrocene-Pd(II) complexes arises from both higher activation enthalpy ($\Delta H^{\ddagger}$) and smaller activation entropy ($\Delta S^{\ddagger}$).

Introduction

The discovery by Brookhart and co-workers[1,2] of versatile, highly active Pd(II) and Ni(II) aryl-substituted α-diimine catalysts **1** has sparked renewed interest in developing late-transition-metal catalysts for olefin polymerization.[3−5] It was proposed that the key to producing high molecular weight polymers by **1** is the incorporation of bulky substituents in the ortho-positions of the aryl rings, which block the axial faces of the square plane and retard the rate of ethylene associative chain transfer. Following Brookhart's original reports, considerable effort has been spent to identify other Ni(II) and Pd(II) complexes bearing bulky bidentate ligands for olefin polymerizations.[6−25] One

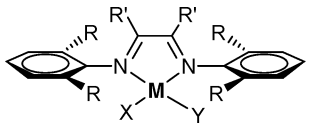

1

M = Ni, Pd

* Corresponding author. E-mail: zguan@uci.edu.

(1) Johnson, L. K.; Killian, C. M.; Brookhart, M. *J. Am. Chem. Soc.* **1995**, *117*, 6414−6415.
(2) Johnson, L. K.; Mecking, S.; Brookhart, M. *J. Am. Chem. Soc.* **1996**, *118*, 267−268.
(3) Ittel, S. D.; Johnson, L. K.; Brookhart, M. *Chem. Rev.* **2000**, *100*, 1169−1203.
(4) Gibson, V. C.; Spitzmesser, S. K. *Chem. Rev.* **2003**, *103*, 283−315.
(5) Younkin, T. R.; Connor, E. F.; Henderson, J. I.; Friedrich, S. K.; Grubbs, R. H.; Bansleben, D. A. *Science* **2000**, *287*, 460−462.
(6) Guan, Z.; Marshall, W. J. *Organometallics* **2002**, *21*, 3580−3586.
(7) Kapteijn, G. M.; Spee, M. P. R.; Grove, D. M.; Kooijman, H.; Spek, A. L.; van Koten, G. *Organometallics* **1996**, *15*, 1405−1413.
(8) Ruelke, R. E.; Kaasjager, V. E.; Wehman, P.; Elsevier, C. J.; van Leeuwen, P. W. N. M.; Vrieze, K.; Fraanje, J.; Goubitz, K.; Spek, A. L. *Organometallics* **1996**, *15*, 3022−3031.
(9) Crociani, L.; Bandoli, G.; Dolmella, A.; Basato, M.; Corain, B. *Eur. J. Inorg. Chem.* **1998**, 1811−1820.
(10) Crociani, L.; Tisato, F.; Refosco, F.; Bandoli, G.; Corain, B. *Eur. J. Inorg. Chem.* **1998**, 1689−1697.
(11) Reddy, K. R.; Surekha, K.; Lee, G.-H.; Peng, S.-M.; Liu, S.-T. *Organometallics*, ASAP.
(12) Reddy, K. R.; Chen, C.-L.; Liu, Y.-H.; Peng, S.-M.; Chen, J.-T.; Liu, S.-T. *Organometallics* **1999**, *18*, 2574−2576.
(13) Reddy, K. R.; Surekha, K.; Lee, G.-H.; Peng, S.-M.; Liu, S.-T. *Organometallics* **2000**, *19*, 2637−2639.
(14) Reddy, K. R.; Surekha, K.; Lee, G.-H.; Peng, S.-M.; Chen, J.-T.; Liu, S.-T. *Organometallics* **2001**, *20*, 1292−1299.
(15) Mueller, C.; Iverson, C. N.; Lachicotte, R. J.; Jones, W. D. *J. Am. Chem. Soc.* **2001**, *123*, 9718−9719.

10.1021/om034051r CCC: $25.00
Publication on Web 10/28/2003

Chart 1

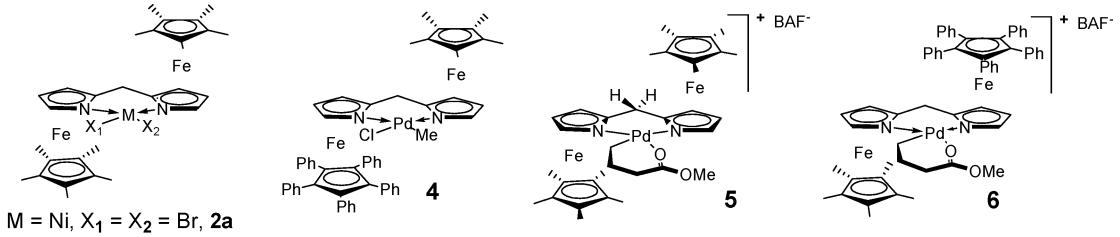

unique feature of the polyolefins formed by the Ni(II)- and Pd(II)-α-diimine catalysts is their branched topologies, which was proposed to be introduced by catalyst isomerization or "walking" along the polyethylene backbone during the migratory insertion polymerization.[1,2,26] By exploiting this chain-walking feature, it was shown that polyethylenes with a broad spectrum of topology ranging from linear to hyperbranched to dendritic can be obtained from polymerization of ethylene by simply varying ethylene pressure.[27−31]

The aim of this study is to explore a new family of bisazaferrocene-based Ni(II) and Pd(II) complexes (**2**−**6** in Chart 1) as potential catalysts for ethylene polymerization. In our plan, we want to explore a different type of bidendate nitrogen donor ligand together with a different type of molecular architecture for shielding the axial faces of the coordination center. We chose bisazaferrocene ligands on the basis of the following three considerations: (1) The two sp^2-hybridized nitrogen atoms in the azaferrocene rings can efficiently chelate to Ni(II) and Pd(II). The relatively good σ-donating ability of azaferrocene nitrogen[32] may result in an improved thermal stability[33] or better tolerance to polar functional groups for the catalysts. (2) Upon coordination with metal ions, the bisazaferrocene molecular architecture should present the bulky pentamethyl or pentaphenyl cyclopentadiene (Cp* or Cp°) rings above and below the coordination plane, which serves as an alternative mode of blocking the associative chain transfer processes of ethylene from the axial faces. (3) The pseudo-C_2 symmetry of the complexes may lead to stereospecific polymerization for α-olefins. Whereas planar-chiral azaferrocene ligands have been applied extensively to asymmetric catalysis,[34−38] to the best of our knowledge, our work represents the first example of exploring bisazaferrocene ligands in olefin polymerization catalysis.

In this paper, we report the synthesis, characterization, and ethylene polymerization properties of a series of novel C_2-symmetric and unsymmetric bisazaferrocene complexes with late transition metals Ni(II) and Pd(II).

Results and Discussion

A. Synthesis of Symmetric and Unsymmetrical Bisazaferrocene Ligands. Synthesis of Symmetrical Bisazaferrocene Ligands 7 and 8. Following literature procedures, the bis(pentamethyl)azaferrocene diastereomers **7** and **8** were prepared by the generation of [Cp*FeCl] in situ followed by treatment with the dilithiated di(2-pyrrole)methane (DPM, **9**) and AgCN in THF (Scheme 1).[36] The reaction was quenched by addition of methanol and 2,2′-dipyridyl (bpy). Purification by flash chromatography with a solvent gradient provided diastereomers **7** and **8** in 65% overall yield with a diastereoselectivity ratio (dr) of 1.5:1.

Synthesis of Unsymmetrical Bisazaferrocene Ligands 12 and 13. The synthesis of a bulkier bisazaferrocene ligand was attempted with the purpose of fully blocking the axial faces of the coordination center.[1,2,39] However, the preparation of bis(pentaphenyl)azaferrocene ligand (**10**) was attempted at various conditions without success. Instead of forming the anticipated product **10**, we only isolated the monosubstituted pentaphenylazaferrocenyl moiety, Cp°FeDPM-H (**11**), in 69% yield (Scheme 2). The failure to form complex **10** was attributed to the high sterics of the pentaphenyl moiety.

Because of the difficulty in obtaining a bis(pentaphenyl)azaferrocene ligand, a less sterically hindered Cp*Fe group was subsequently introduced to the free pyrrole ring of **11** to obtain an unsymmetrical Cp*Cp°Fe_2DPM

(16) Ikeda, S.; Ohhata, F.; Miyoshi, M.; Tanaka, R.; Minami, T.; Ozawa, F.; Yoshifuji, M. *Angew. Chem., Int. Ed.* **2000**, *39*, 4512−4513.
(17) Rachita, M. J.; Huff, R. L.; Bennett, J. L.; Brookhart, M. *J. Polym. Sci., Part A: Polym. Chem.* **2000**, *38*, 4627−4640.
(18) Lee, B. Y.; Bazan, G. C.; Vela, J.; Komon, Z. J. A.; Bu, X. *J. Am. Chem. Soc.* **2001**, *123*, 5352−5353.
(19) Daugulis, O.; Brookhart, M. *Organometallics* **2002**, *21*, 5926−5934.
(20) Daugulis, O.; Brookhart, M.; White, P. S. *Organometallics* **2002**, *21*, 5935−5943.
(21) Jenkins, J. C.; Brookhart, M. *Organometallics* **2003**, *22*, 250−256.
(22) Shen, H.; Jordan, R. F. *Organometallics* **2003**, *22*, 1878−1887.
(23) Foley, S. R.; Stockland, R. A., Jr.; Shen, H.; Jordan, R. F. *J. Am. Chem. Soc.* **2003**, *125*, 4350−4361.
(24) Gibson, V. C.; Tomov, A. *Chem. Commun.* **2001**, 1964−1965.
(25) Schmid, M.; Eberhardt, R.; Klinga, M.; Leskela, M.; Rieger, B. *Organometallics* **2001**, *20*, 2321−2330.
(26) Moehring, V. M.; Fink, G. *Angew. Chem.* **1985**, *97*, 982−984.
(27) Guan, Z.; Cotts, P. M.; McCord, E. F.; McLain, S. J. *Science* **1999**, *283*, 2059−2062.
(28) Guan, Z. *Chem.−Eur. J.* **2002**, *8*, 3086−3092.
(29) Chen, G.; Ma, X. S.; Guan, Z. *J. Am. Chem. Soc.* **2003**, *125*, 6697−6704.
(30) Guan, Z. *J. Am. Chem. Soc.* **2002**, *124*, 5616−5617.
(31) Cotts, P. M.; Guan, Z.; McCord, E.; McLain, S. *Macromolecules* **2000**, *33*, 6945−6952.
(32) Silver, J.; Zakrzewski, J.; Tosik, A.; BukowskaStrzyzewska, M. *J. Organomet. Chem.* **1997**, *540*, 169−174.
(33) Moody, L. S.; MacKenzie, P. B.; Killian, C. M.; Lavoie, G. G.; Ponasik, J. A., Jr.; Smith, T. W.; Pearson, J. C.; Barrett, A. G. M. PCT Int. Appl. WO 0222694, 2002.
(34) Ruble, J. C.; Fu, G. C. *J. Org. Chem.* **1996**, *61*, 7230−7231.
(35) Dosa, P. I.; Ruble, J. C.; Fu, G. C. *J. Org. Chem.* **1997**, *62*, 444−445.
(36) Lo, M. M. C.; Fu, G. C. *J. Am. Chem. Soc.* **1998**, *120*, 10270−10271.
(37) Hodous, B. L.; Ruble, J. C.; Fu, G. C. *J. Am. Chem. Soc.* **1999**, *121*, 2637−2638.
(38) Fu, G. C. *Acc. Chem. Res.* **2000**, *33*, 412−420.
(39) Mecking, S.; Johnson, L. K.; Wang, L.; Brookhart, M. *J. Am. Chem. Soc.* **1998**, *120*, 888−899.

Scheme 1

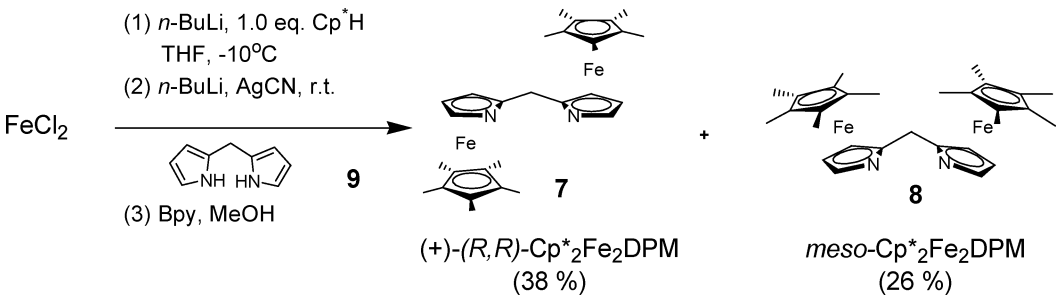

Scheme 2

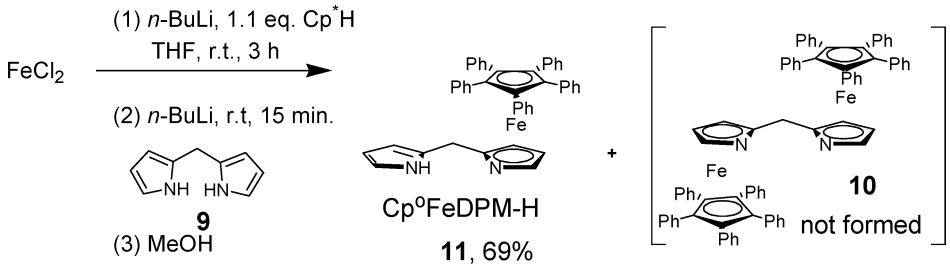

Scheme 3

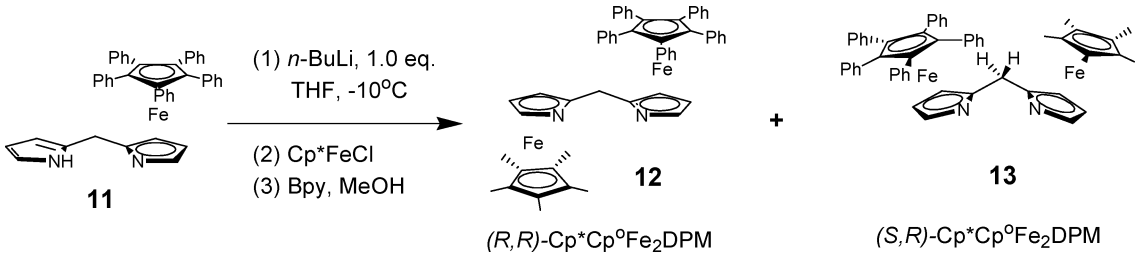

Scheme 4

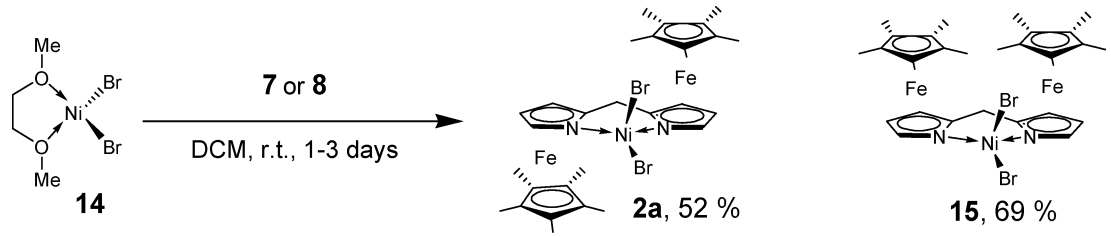

ligand (**12**, Scheme 3). The reaction gave two diastereomers **12** and **13** in equal amount. Previous reports have shown that introduction of a silver reagent during the course of a reaction improved the dr for a similar kind of bisazaferrocene synthesis.[36] It was postulated that an energetically favorable semirigid six-membered silvercyclic transition state was formed to promote a favorable attack below the plane of pentamethylazaferrocene due to steric repulsion.[40] Various metal ions including $ZnCl_2$, AgOAc, and AgCN were added to the reaction solution after the lithiation of **11** (step 1 in Scheme 3). However, the dr improvement was rather modest with 1.3:1 as the highest obtained for **12** and **13**. The two diastereomers were conveniently separated by flash column chromatography. The syn- and anti-stereoisomers are assigned on the basis of the characteristic NMR features for the bridging methylene protons: the chemical shifts for the two diastereotopic protons on the methylene bridge have larger chemical shift differences for the syn-isomer **13** than for the anti-isomer **12**.

B. Synthesis and Characterization of Ni(II) and Pd(II) Complexes with the Bisazaferrocene Ligands. Synthesis of $NiBr_2$ and $PdCl_2$ Complexes with the Symmetrical Bisazaferrocene Ligand as Precatalysts. First, $NiBr_2$ complexes with the symmetrical bisazaferrocene ligand **7** or **8** were prepared according to modified literature procedures.[1] The (DME)-$NiBr_2$ complex (**14**) was added to a solution of either **7** or **8** in dichloromethane (Scheme 4). Concentrated solution of **2a** or **15** was precipitated with hexanes to afford **2a** or **15** in 52% or 69% yields, respectively.

Due to the paramagnetic nature of the $NiBr_2$ complexes, satisfactory NMR spectra could not be obtained for complexes **2a** and **15**, which were instead characterized by combustion analysis. Fortunately, good quality single crystals of **2a** were obtained from a concentrated chloroform solution layered with hexanes. The X-ray

(40) O'Connor, J. M.; Casey, C. P. *Chem. Rev.* **1987**, *87*, 307−318.

Scheme 5

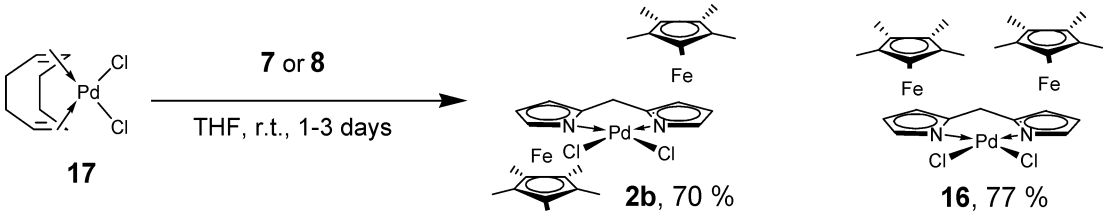

Scheme 6

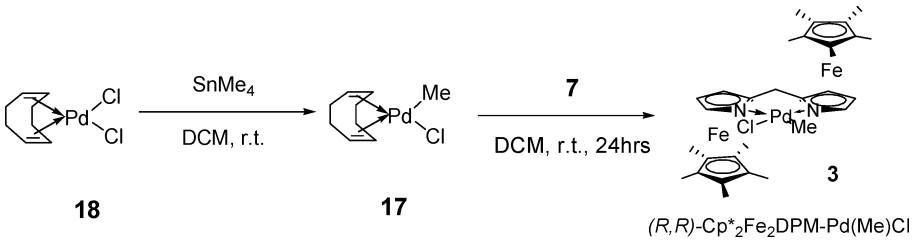

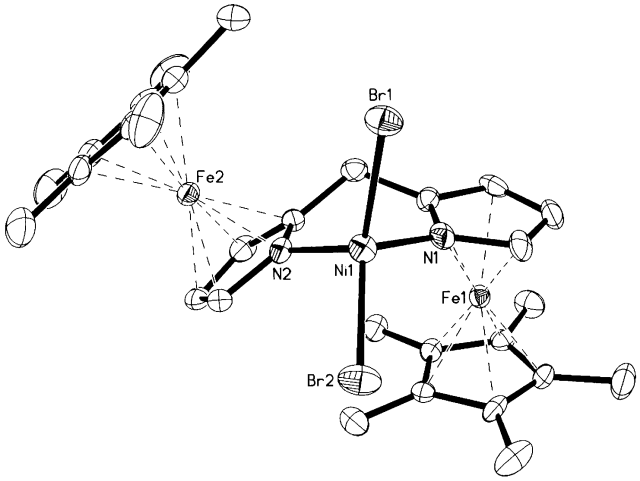

Figure 1. ORTEP view of **2a** showing important atoms labeled. Selected interatomic distances (Å) and angles (deg): Ni(1)−N(2) = 1.986(4), Ni(1)−N(1) = 1.990(5), Ni(1)−Br(2) = 2.3643(9), Ni(1)−Br(1) = 2.3794(9), N(2)−Ni(1)−N(1) = 92.09(18), Br(2)−Ni(1)−Br(1) = 121.25(3), N(2)−Ni(1)−Br(2) = 106.85(13), N(1)−Ni(1)−Br(2) = 116.15(14), N(2)−Ni(1)−Br(1) = 117.92(13), N(1)−Ni(1)−Br(1) = 98.83(13), Cnt1−Fe(1)−Cnt2 = 175.5, Cnt3−Fe(2)−Cnt4 = 176.2.

crystal structure of **2a** was successfully solved as shown in Figure 1 together with selected bond distances and angles.

The bisazaferrocene-Ni(II) complex **2a** is pseudo-C_2 symmetrical, and the Ni coordination assumes a pseudo-tetrahedral geometry with a boatlike conformation for the six-membered coordination ring. The N−Ni and Ni−Br bond distances of the complex **2a** are very close to the values observed in the α-diimine analogues.[41,42] However, in contrast to the α-diimine $NiBr_2$ complex having bulky R substituents (**1**), the pentamethylazaferrocene moieties may not sufficiently block the axial faces of the coordination center for complex **2a**. Instead of being parallel to each other, the two Cp* rings are titled with a torsion angle of 168.8° between them, presumably caused by the steric repulsion between the Br atoms with the Cp* rings. As shown by Brookhart and co-workers in previous studies of Ni(II)- and Pd(II)-α-diimine complexes, blocking axial faces of the coordination site with bulky substituents of the aniline moieties is critical for preventing an associative chain transfer process in order to form high molecular weight polymers. Because of the exposed axial faces in the bisazaferrocene complex, the metal center could be susceptible to ethylene associative chain transfer processes, which may contribute at least partially to the formation of relatively low molecular weight PEs in the ethylene polymerization catalyzed by the these complexes (vide infra). Another notable difference between the two complexes is the bite angle of the two nitrogens. While the α-diimine $NiBr_2$ complexes generally have bite angles of 82.4−82.6°, the complex **2a** has a bite angle of 92.1°, which is almost 10° larger than the α-diimine analogues.[41,42]

Complexes of $PdCl_2$ with the symmetric bisazaferrocene, **2b** and **16**, were synthesized by combining and modifying the procedures of Brookhart and Fu et al.[1,36] The syntheses were accomplished by ligand substitution of (COD)Pd(Me)Cl (**17**) with **7** or **8** (Scheme 5). After recrystallization from hexanes, the complexes **2b** and **16** were obtained in 70% and 77% yields, respectively. Complexes **2b** and **16** were characterized by ^{1}H and ^{13}C NMR spectroscopy, high-resolution mass spectrometry (HRMS), and combustion analyses.

Synthesis of Preactivated Pd(II) Complexes with the Symmetric Bisazaferrocene Ligand 7. Because of the low polymerization activities observed for the $NiBr_2$ and $PdCl_2$ complexes (**2a**,**b**, **15**, **16**) upon MAO activation, in later studies we focused on the syntheses and polymerization studies of Pd(II) complexes in preactivated forms. First, the Pd(Me)Cl-bisazaferrocene complex **3** was prepared according to a modified literature procedure.[43] The (COD)$PdCl_2$ (**18**) was first converted into (COD)Pd(Me)Cl (**17**), which was subsequently complexed to the C_2-symmetrical bisazaferrocene ligand **7** to afford **3** in 84% yield (Scheme 6).

The complex **3** was then activated with sodium tetrakis[3,5-bis(trifluoromethyl)phenyl]borate (NaBAF, **19**) in the presence of diethyl ether (Et_2O) or acetonitrile

(41) Gates, D. P.; Svejda, S. K.; Onate, E.; Killian, C. M.; Johnson, L. K.; White, P. S.; Brookhart, M. *Macromolecules* **2000**, *33*, 2320−2334.
(42) Maldanis, R. J.; Wood, J. S.; Chandrasekaran, W. A.; Rausch, M. D.; Chien, J. C. W. *J. Organomet. Chem.* **2002**, *645*, 158−167.
(43) Rulke, R. E.; Ernsting, J. M.; Spek, A. L.; Elsevier, C. J.; Vanleeuwen, P.; Vrieze, K. *Inorg. Chem.* **1993**, *32*, 5769−5778.

Scheme 7

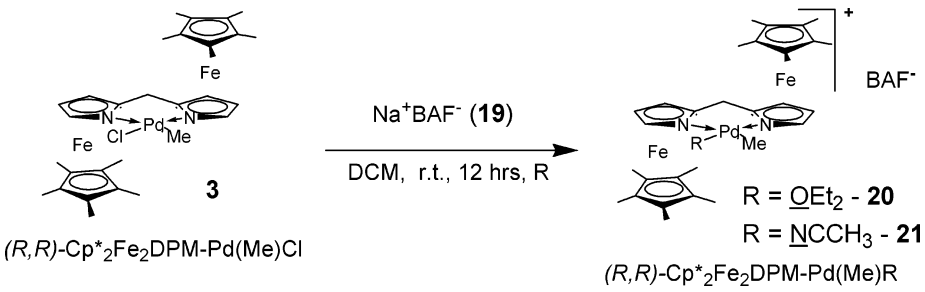

Scheme 8

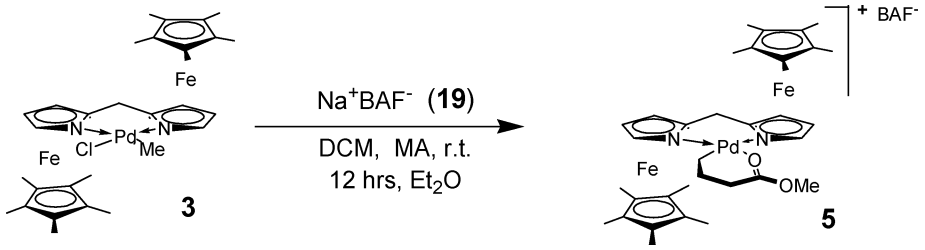

Scheme 9

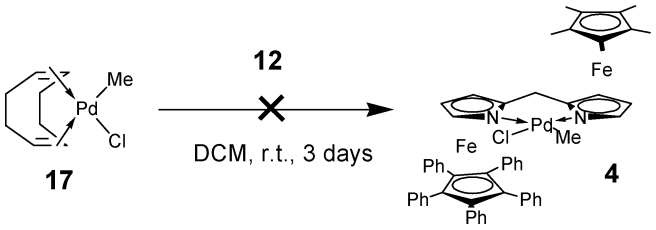

Scheme 10

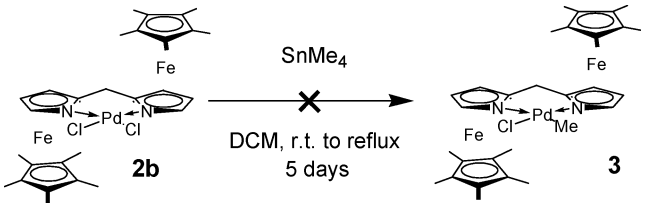

(ACN) as stabilizers.[1,2] While the ether-stabilized Pd salt $[Cp^*_2Fe_2DPMPd(Me)OEt_2]^+BAF^-$ (**20**) was unstable as shown by ^1H NMR, the ACN-stabilized Pd salt $[Cp^*_2Fe_2DPMPd(Me)NCCH_3]^+BAF^-$ (**21**) was sufficiently stable to be isolated as brittle dark red crystals in 91% yield (Scheme 7).[1,44] Complex **21** was fully characterized by HRMS, combustion analysis, and ^1H and ^{13}C NMR.

Another preactivated Pd(II) complex, a palladacyclic derivative $[Cp^*_2Fe_2DPMPd(CH_2)_3COOMe^+]BAF^-$ (**5**), was synthesized by activating complex **3** with NaBAF followed by the addition of methyl acrylate (MA).[2] The complex was characterized by ^1H and ^{13}C NMR, HRMS, and combustion analysis.

Synthesis of Preactivated Pd(II) Complexes with the Unsymmetrical Bisazaferrocene Ligand 12. We initially attempted to synthesize the unsymmetrical Cp°Cp*Fe_2DPM-Pd(Me)Cl complex **4** by following the same route used in the synthesis of complex **3**. Unfortunately, the displacement of COD in **17** by the unsymmetrical ligand **12** did not occur, which was presumably caused by the steric hindrance of the bulky unsymmetrical azaferrocene ligand **12** (Scheme 9).

An alternative route that involves a direct methylation of a $PdCl_2$-bisazaferrocene complex with tetramethyltin ($SnMe_4$) to form the Pd(Me)Cl complex was pursued next. The symmetric $Cp^*_2Fe_2DPMPdCl_2$ complex (**2b**) was used as a model system to investigate the feasibility of this route. Shown by MS and ^1H NMR, the transmetalation reaction to **2b** did not occur at various conditions (Scheme 10). We speculate that the nonreactivity of complex **2b** toward $SnMe_4$ may arise from a destabilizing trans-ligand effect.[45] Since the methyl group is known to be an excellent σ-donor, the exchange of a weaker σ-donating Cl atom with a methyl group on the Pd(II) center should result in a destabilizing trans-effect because the pentamethylazaferrocene ligand has good σ-donating capability.[32,45]

To overcome the difficulty encountered in the synthesis of the Pd(Me)Cl complexes **3** and **4**, we developed a new methodology for the synthesis of Pd(Me)Cl complexes. In this approach, a Pd(II) precursor $(PhCN)_2PdCl_2$ (**22**), containing a more labile benzonitrile (PhCN) ligand, was used to generate a transient $[(PhCN)_2Pd(Me)Cl]$ species as a reactive intermediate. Direct ligand substitution in situ then leads to the formation of the desired Pd(Me)Cl complexes. Because of its low stability, the $(PhCN)_2Pd(Me)Cl$ species has to be generated at low temperature under argon followed by in situ ligand substitution within a short period of time. We first employed α-diimine ligand **23** as a model to investigate the feasibility and to optimize the reaction conditions (Scheme 11).

As shown in Scheme 11, the product yield had a strong dependence on the reaction time for the in situ generation of the $(PHCN)_2Pd(Me)Cl$ species. High product yield was obtained at shorter reaction times, which suggests the decomposition of the $(PhCN)_2Pd(Me)Cl$ species even at low temperatures.

Following successful model reaction studies, we applied this methodology to the synthesis of complex **4**. After optimization of reaction conditions, complex **4** was

(44) Bahr, S. R.; Boudjouk, P. *J. Org. Chem.* **1992**, *57*, 5545−5547.

(45) James, P. C.; Hededus, L. S.; Norton, J. R.; Finke, R. G. *Principles and Applications of Organotransition Metal Chemistry*; 1987.

Scheme 11. Model Reaction for in Situ Generation of Pd(Me)Cl Complex (6)

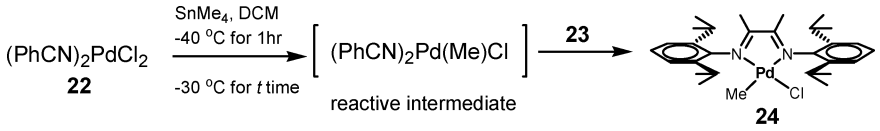

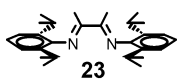

t (hr)	yield
18	28%
4.0	68%
1.5	97%

Scheme 12

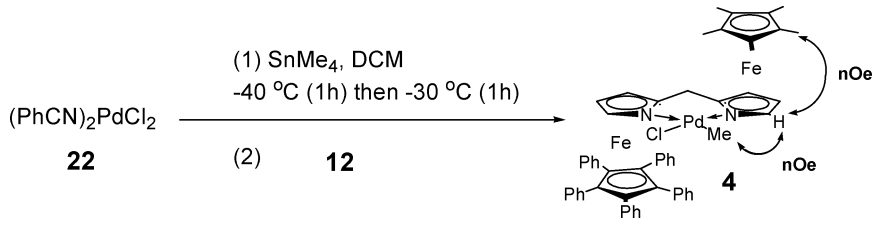

Scheme 13

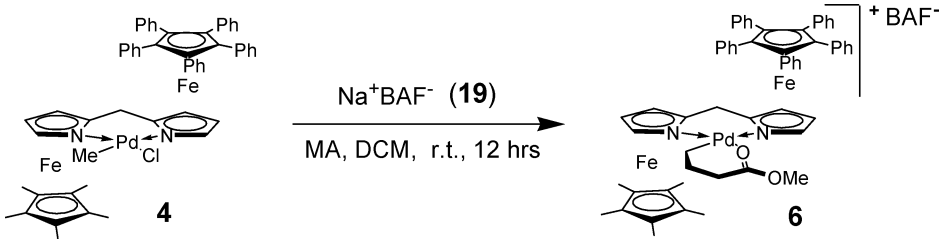

obtained in 77% yield as pink crystals and was characterized by ^{1}H and ^{13}C NMR, HRMS, and combustion analysis. In complex **4**, the regiochemistry of the methyl group being trans to the Cp° azaferrocene was established by Nuclear Overhausser Effects (NOE) on the Pd-Me with the adjacent α-proton on the pyrrole ring (Scheme 12). The regioselectivity of the reaction is attributed to trans ligand effects.[45] Because of inductive and resonance stabilization of the phenyl groups, the Cp° azaferrocene has significantly less σ-donating ability than the pentamethyl azaferrocene moiety. Therefore, the strong σ-donating methyl group prefers to stay trans to the Cp° azaferrocene moiety.

With complex **4** in hand, the synthesis of {Cp°Cp*Fe_2-DPM-Pd[$(CH_2)_3$COOMe]}$^+$BAF$^-$ (**6**) was carried out by following the same procedure as described previously in the synthesis of complex **5**. Immediately after the addition of NaBAF into complex **4** in DCM, MA was added and the solution was allowed to stir at room temperature overnight to afford complex **6** in 89% yield as dark red crystals (Scheme 13). The complex **6** was characterized by ^{1}H and ^{13}C NMR, HRMS, and combustion analysis.

C. Oligomerization of Ethylene with the Pd^{II} and Ni^{II} Bisazaferrocene Complexes. $NiBr_2$ and $PdCl_2$ Complexes. The ethylene polymerization reactions were carried out in a 600 mL Parr reactor using toluene as the solvent. For all $NiBr_2$ and $PdCl_2$ complexes (**2a**,**b**, **15**, and **16**) methylaluminoxane (MAO) was used to activate the catalyst precursors for polymerization of ethylene. Unfortunately, all these complexes upon activation with MAO exhibited very low activities. Polymerization reactions at various temperatures, ethylene pressures, and varying Al/metal ratios afforded only trace amount of polymers. For the $PdCl_2$ complex, black Pd dust was observed after terminating the polymerization, indicating the decomposition of the Pd species upon activation. For $NiBr_2$ complexes, no direct evidence of catalyst decomposition was observed. While the reason for the very low activities of these complexes activated by MAO is still unknown, we speculate the highly reactive MAO may interact with the azaferrocene ligand to cause the catalyst deactivation. To avoid the use of MAO, we then focused on developing Pd(II)-bisazaferrocene catalysts that are already in active form with no need of further activation.

The preactivated Pd(II) complexes **5** and **6** were selected to test for ethylene polymerization at various ethylene pressures and temperatures. The polymerization data are summarized in Table 1. The pseudo-C_2-symmetric complex **5** polymerized ethylene to form oligomers (number-averaged molecular weight, M_n, about 200−600 g/mol) with moderate branching (20−60 br./1000C) (Table 1). Both the polymerization activity as measured by turnover frequency (TOF) and the PE molecular weight are significantly lower than the values obtained with the Pd(II)-α-diimine analogues.[1,2,46]

Ethylene polymerizations using complex **5** were first run at different temperatures ranging from 20 to 120 °C while maintaining all other parameters constant (entries 1−6). The catalyst productivity increases ini-

(46) Tempel, D. J.; Johnson, L. K.; Huff, R. L.; White, P. S.; Brookhart, M. *J. Am. Chem. Soc.* **2000**, *122*, 6686−6700.

Table 1. Ethylene Oligomerization Data by Catalysts 5 and 6[a]

entry	catalyst	loading (μmol)	pressure (psig)	temp (°C)	time (h)	yield of polymer (g) [b]	TOF[c]	M_n[d]	branch/ 1000 C [d]
1	**5**	13	100	20	2.5	0.055	60	598	50
2	**5**	13	100	40	2.5	0.152	167	424	45
3	**5**	13	100	60	2.5	0.423	465	318	41
4	**5**	13	100	80	2.5	1.89	2080	235	29
5	**5**	13	100	100	2.5	1.47	1615	233	38
6	**5**	13	100	120	2.5	0.903	992	230	36
7	**5**	14	50	80	2.5	0.838	855	226	43
8	**5**	14	200	80	2.5	1.30	1330	242	28
9	**5**	12	500	80	2.5	2.61	3110	236	27
10	**6**	6	100	20	24	0.048	13	270	33
11	**6**	11	100	40	24	0.400	54	186	19
12[e]	**6**	12	100	80	2.5	0.017	20	247	60

[a] General polymerization procedure: 70 mL of toluene, 6−14 μmol of catalyst unless specified. [b] Yield of PE may not accurately reflect the true activity due to the removal of volatile oligomers during workup. [c] TOF = turnover frequency per hour, i.e., moles of ethylene consumed in formation of PE per mole of catalyst per hour. [d] M_n and branching density were calculated on the basis of ^{1}H NMR according to Brookhart et al.[47] [e] Polymerization was carried out in DCM.

Scheme 14

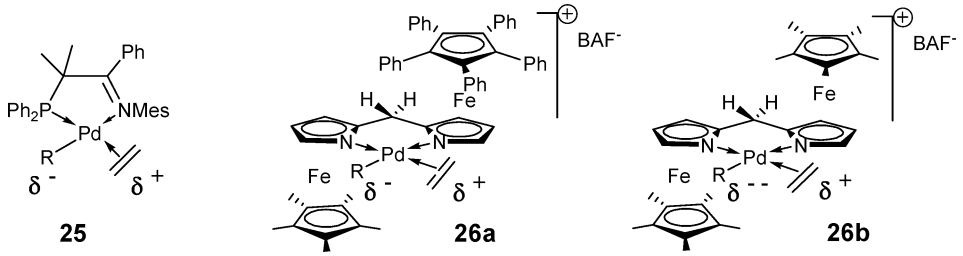

tially with temperature and reaches a maximum around 80 °C. As the temperature was further raised, the activity starts to drop, indicating catalyst deactivation at higher temperature. Nevertheless, the catalyst remains active even at 120 °C to polymerize ethylene for many hours. This is in sharp contrast to the Pd(II)-α-diimine counterparts, which is known to decompose rapidly at about 50 °C.[46] Increase of temperature resulted in a decrease in M_n, which is typical for transition-metal-catalyzed olefin polymerizations due to increased rate of chain transfer reactions at elevated temperatures. The molecular weights of the PEs obtained with **5** are generally low compared to those obtained with the Pd(II)-α-diimine catalysts. Whereas the exact cause for this is yet to be understood, based on the X-ray crystal structure of complex **2a** (Figure 1), we tentatively attributed this partially to the openness of the axial faces of complex **5** (vide supra). The easy access by ethylene from the axial faces makes the catalyst susceptible to ethylene associative chain transfer. The ^{1}H NMR spectra of the PE products showed that they contain a significant portion of internal olefins, which could self-inhibit the catalyst and partially suppress the intrinsic catalytic activity of the catalyst.

Oligomerizations were then carried out at 80 °C with three pressures (Table 1, entries 7−9). An increase in pressure resulted in an increase in productivity (TOF) but a decrease in branching density, both consistent with the Pd(II)-α-diimine systems.[46] The branches in the PEs were presumably formed by the chain-walking mechanism proposed by Brookhart and Fink for the Ni(II) and Pd(II) catalyst systems.[1,2,26]

Oligomerization of ethylene with complex **6** was carried out and compared to the symmetrical analogue, **5** (Table 1, entries 10−12). The unsymmetrical complex **6** was considerably less active in polymerizing ethylene than the symmetrical complex **5**. In addition, the unsymmetrical catalyst **6** appears to be less thermally stable than the symmetrical analogue **5**, as evident with the drop of TOF at 40 °C and the observed formation of Pd dust during polymerization. The significantly lower activity for the unsymmetrical catalyst **6** than the symmetric catalyst **5** is analogous to the comparison between the reported unsymmetrical Pd(II)-phosphine-imine (P∧N) complex **25** and its symmetrical Pd(II)-α-diimine complexes.[19] It was shown that the unsymmetrical P∧N complexes with Ni(II) and Pd(II) were less reactive than their symmetrical α-diimine or α-diphosphine counterparts. The migratory insertion barrier for the unsymmetrical complex **25** was shown to be 7.4 kcal/mol higher than the barrier for either the α-diimine or α-diphosphine analogues. The lower reactivity of our unsymmetrical complex **6** than the symmetrical one **5** can be explained by the same arguments used to explain the low reactivity of other unsymmetrical complexes.[19,45] As shown in Scheme 14, the situation is unfavorable for migratory insertion for the unsymmetrical complex in its more stable resting state **26a**. In simple view, the migratory insertion can be regarded as an attack of the nucleophilic R group on the electrophilic ethylene ligand. The R group in **26a** (trans to Cp° azaferrocene) is less nucleophilic than the R group in the symmetric complex **26b** (trans to Cp* azaferrocene). Therefore, the nucleophilic addition of R to ethylene (equivalent to migratory insertion) is slower for the unsymmetrical complex **26a**.[19,45]

D. Kinetic Investigation of Methyl Migration and Ethylene Consumption. To understand why the bisazaferrocene catalysts exhibit lower polymerization activities than their α-diimine counterparts, kinetic studies on methyl migration and subsequent ethylene consumption for complex **27** were carried out and the

Scheme 15

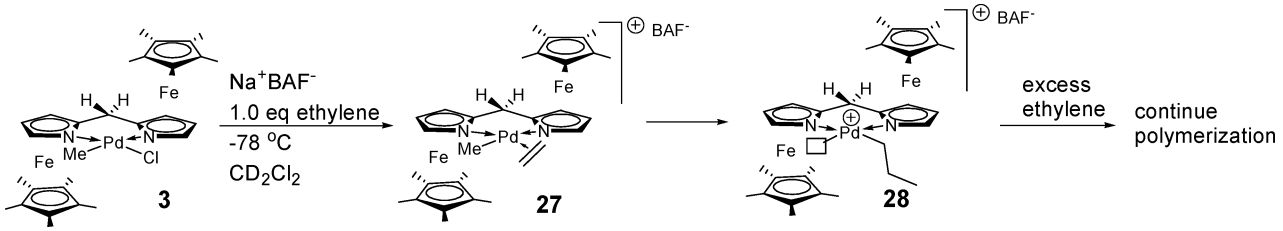

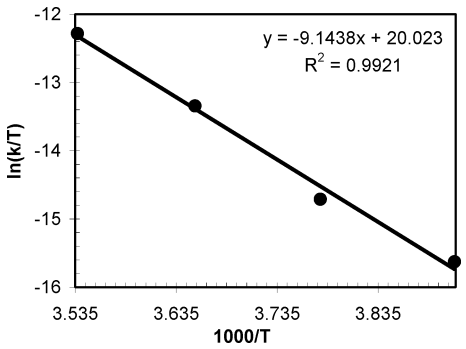

Figure 2. Eyring plot for subsequent ethylene insertion by complex **27**.

Scheme 16

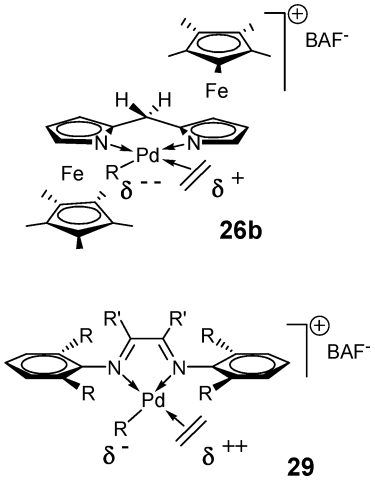

data were compared to those of the bisimine analogues.[1,46,47] The complex **3** was activated in an NMR tube with NaBAF at −78 °C and then complexed with ethylene to form the Pd(Me)(H_2C=CH_2) complex (**27**). After warming up to −14 °C, the first-order kinetics of the first methyl migration was monitored by the decrease of the Pd-Me group with time (Scheme 15):

The first-order rate constant for the first methyl migration was determined to be $k = 2.49 \times 10^{-5}$ s^{-1} at −14 °C, which corresponds to a $\Delta G^{\ddagger}$ of 20.6 kcal/mol using the Eyring equation. This insertion barrier for the first methyl migration of complex **27** is about 2−3 kcal/mol higher than the values of the Pd(II)-α-diimine analogues for which the $\Delta G^{\ddagger}$ is in the range 17.5−18.8 kcal/mol.[1] The rate of subsequent insertions was modeled by the zero-order kinetics of ethylene disappearance at 9.5 °C, $k = 1.3 \times 10^{-3}$ s^{-1}, corresponding to a $\Delta G^{\ddagger} =$ 20.2 kcal/mol (Scheme 15). Again, this energetic barrier is 2−3 kcal/mol higher than the values for the bisimine analogues, for which the $\Delta G^{\ddagger}$ is usually in the range 16.9−17.6 kcal/mol.[1] A $\Delta\Delta G^{\ddagger}$ of 2−3 kcal/mol corresponds to about 2 orders of magnitude difference in rate at room temperature, which agrees qualitatively with the observed difference in polymerization activities between the Pd(II)-bisazaferrocene complexes and the Pd(II)-α-diimine counterparts. Furthermore, the ethylene consumption rates for complex **27** were measured at various temperatures ranging from 255.7 to 282.7 K. An Erying plot (Figure 2) gives $\Delta H^{\ddagger} = 18.2$ kcal/mol and $\Delta S^{\ddagger} = -7.4$ eu. This $\Delta H^{\ddagger}$ value is considerably higher than the values for the Pd(II)-α-diimine counterparts (14.2 kcal/mol), while the $\Delta S^{\ddagger}$ value is smaller than the values for the Pd(II)-α-diimine counterparts (−11.2 eu).[46] Therefore, the ethylene insertion by Pd(II)-bisazaferrocene complex **27** is unfavorable from both enthalpic and entropic considerations, which explains why the Pd(II)-bisazaferrocene complexes exhibit much lower reactivity than the α-diimine counterparts. The higher insertion barrier for the Pd(II)-bisazaferrocene complex than for the α-diimine analogues could be the result of a combination of both electronic and steric effects. Electronically (Scheme 16), the better σ-donating ability of bisazaferrocene should make the R group more nucleophilic but the coordinated ethylene less electrophilic for **26b** than for α-diimine complex **29**. The net result of these two countereffects is not obvious, however. Sterically, both experimental[46] and theoretical calculation[48] results have shown that bulkier α-diimine complexes exhibit lower insertion barriers because steric congestion causes ground state destabilization for the resting complex **29**. The rather open structure of the bisazaferrocene complex **26b** around the coordination center makes the resting state relatively stable in the ground state, which should lead to a larger activation energy as it proceeds to its transition state.

Conclusions

A series of novel nickel and palladium complexes with symmetrical and unsymmetrical bisazaferrocene catalysts were successfully synthesized and characterized, and some were tested for ethylene polymerization. The X-ray crystal structure for the bisazaferrocene-$NiBr_2$ complex (**2a**) shows it as a pseudo-C_2-symmetrical complex with the Ni coordination center assuming a pseudo-tetrahedral geometry. The titled Cp* rings leave the coordination center susceptible to associative chain transfer processes, which may partially contribute to the low molecular weights in their ethylene polymerizations. Because the bisazaferrocene complexes with simple Ni(II) and Pd(II) halides (**2a**,**b**, **15**, and **16**) gave only a trace amount of PE upon activation with MAO, our

(47) Daugulis, A.; Brookhart, M.; White, P. S. *Organometallics* **2002**, *21*, 5935−5943.

(48) Deng, L.; Woo, T. K.; Cavallo, L.; Margl, P. M.; Ziegler, T. *J. Am. Chem. Soc.* **1997**, *119*, 6177−6186.

investigation then turned its focus on the development and ethylene polymerization studies of preactivated symmetrical and unsymmetrical Pd(II)-bisazaferrcoene complexes (**5, 6,** and **21**). Complex **5** and **21** were synthesized in straightforward routes by first forming the appropriate Pd(Me)Cl complexes through simple ligand substitution followed by activation with NaBAF in the presence of various stabilizers. However, significant difficulty was encountered in the preparation of the unsymmetrical bisazaferrocene complex **6** due to steric and electronic factors, which prompted us to investigate alternative routes to achieve the synthetic goal. A novel route was successfully developed to make Pd(Me)Cl complexes with various dinitrogen ligands by generating a transient $[(PhCN)_2Pd(Me)Cl]$ species in situ followed by ligand substitution reaction. Utilizing this new methodology, the unsymmetrical azaferrocene complex **6** was obtained in good yield.

Preactivated complexes **5** and **6** were selected to test for ethylene polymerization at various conditions. They both gave oligomeric PEs with M_n in the range of 200−600 g/mol and branching density from 20 to 60 br./1000 carbons. The symmetrical complex **5** has demonstrated a higher productivity than the unsymmetrical complex **6**, but both are significantly less productive than the α-diimine counterparts. One unique feature is that their thermal stability is considerably higher than the α-diimine counterparts: for example, *complex **5** remained active in ethylene polymerization at temperatures as high as 120 °C*. The formation of low molecular weight oligomers may be partially due to the openness of the axial faces of the coordination center, as shown by the X-ray structure of the $NiBr_2$ complex (**2a**). The significantly lower activity for the unsymmetrical catalyst **6** than the symmetric catalyst **5** is analogous to the difference in activities between the reported unsymmetrical Pd(II)-phosphine-imine (P∧N) complex **25** and its symmetrical Pd(II)-α-diimine complex. The observation was explained by the same electronic arguments (trans ligand effects) used to explain the low reactivity of other unsymmetrical complexes.

To understand why the bisazaferrocene catalysts exhibit much lower polymerization activities than their α-diimine counterparts, kinetic studies on methyl migration and subsequent ethylene consumption for complex **27** were carried out and the data were compared to those of the α-diimine analogues. Low-temperature NMR experiments revealed that the insertion barriers for both the first methyl migration and subsequent ethylene insertion by complex **27** are 2−3 kcal/mol higher than the values obtained for the Pd(II)-α-diimine analogues, which corresponds to about 2 orders of magnitude difference in rate at room temperature. This agrees qualitatively with the observed difference in polymerization activities between the Pd(II)-bisazaferrocene complexes and the Pd(II)-α-diimine counterparts. Further kinetic studies at various temperatures reveal that ethylene insertion by Pd(II)-bisazaferrocene complexes is unfavorable from both enthalpic and entropic considerations. These kinetic data explain why the Pd(II)-bisazaferrocene complexes exhibit much lower reactivity than the diimine counterparts.

Experimental Section

General Procedure. All metal-related reactions were initially weighed and carried out in a Vacuum Atmospheres glovebox filled with nitrogen, unless otherwise noted. All other moisture and air-sensitive reagents were carried out in either oven-dried (180 °C) or flame-dried glassware using magnetic stirring under positive pressure of argon or nitrogen. Flash chromatography with unbound azaferrocene ligands was carried out using forced flow under nitrogen with Silicycle 230−400 mesh (pH 5.5−6.5) silica gel. All other flash chromatography was performed using forced flow under nitrogen with EM Science 230−400 mesh silica gel, unless otherwise noted. NMR spectra were recorded on Bruker DRX400, Bruker GN500, and Bruker Omega500 MHz FT-NMR instruments. Proton and carbon NMR spectra were recorded in ppm and were referenced to indicated solvents. Data were reported as follows: chemical shift, multiplicity (s = singlet, d = doublet, t = triplet, q = quartet, m = multiplet), coupling constant(s) in hertz (Hz), and integration. Multiplets (m) were reported over the range (ppm) at which they appear at the indicated field strength. Mass spectra were obtained on an ES/MS, a VG Analysis 7070E, or a Fisons Autospec spectrometer and were obtained by peak matching. Elemental analysis was performed by Atlantic Microlabs in Marietta, GA. Number average molecular weights (M_n) and degree of branching of the polymer samples were determined by ^1H NMR spectra by following literature procedures.[47] THF, toluene, dichloromethane (DCM), and diethyl ether were degassed under argon and passed through an alumina-packed filtration system. Unless otherwise stated, all reagents were purchased from commercial suppliers and used as received. Pyrrole was distilled under reduced pressure and stored over 4 Å molecular sieves in glovebox at −35 °C. Di(2-pyrrole)methane (DPM) was synthesized according to the procedure by Ka et al.[49] NaBAF was obtained from the procedure by Bahr et al.[44] Ethylene polymerization is performed by using a 600 mL Parr high-pressure reactor with an overhead mechanical stirrer and temperature control.

General Procedure A: Synthesis of Complexes with Metal Halides.[36,50−53] To a solution of ±-(*S*,*S*)- and (*R*,*R*)-Cp*$_2$Fe$_2$DPM or *meso*-Cp*$_2$Fe$_2$DPM dissolved in THF or DCM (0.3 M relative to ligand) was added the metal halide (MX_2) (the ligand:M was typically in the range 1.05−1.15:1). The solution was stirred at rt for at least 24 h in the glovebox. The solution was filtered through Celite, concentrated, and precipitated by layering with hexanes, unless otherwise noted. The metal complex was washed with 3 × 2 mL of hexanes and dried in vacuo overnight, unless otherwise noted.

General Procedure B: Synthesis of Preactivated Pd^{II} Complexes.[36,50−53] To a solution of Cp*$_2$Fe$_2$DPM-Pd(Me)Cl (**3**) or Cp°Cp*Fe$_2$DPM-Pd(Me)Cl (**4**) dissolved in DCM was added an appropriate amount of NaBAF, which was followed immediately by the addition of a stabilizer (Et_2O, ACN, or MA). The resulting solution was stirred at rt for at least 12 h in the glovebox. The salt was filtered through a fine frit filter and dried in vacuo overnight to give a preactivated Pd^{II} salt.

General Procedure C: Ethylene Polymerization by MAO-Activated Complexes. Approximately 10 mg of catalyst was suspended or dissolved in 50 mL of toluene. The resulting toluene suspension or solution was loaded into a 600 mL Parr reactor purged under nitrogen, followed by addition of 20 mL of toluene. After the reactor was purged with 50 psi

(49) Ka, J. W.; Lee, C. H. *Tetrahedron Lett.* **2000**, *41*, 4609−4613.
(50) Killian, C. M.; Johnson, L. K.; Brookhart, M. *Organometallics* **1997**, *16*, 2005−2007.
(51) Small, B. L.; Brookhart, M. *J. Am. Chem. Soc.* **1998**, *120*, 7143−7144.
(52) Small, B. L.; Brookhart, M.; Bennett, A. M. A. *J. Am. Chem. Soc.* **1998**, *120*, 4049−4050.
(53) Gibson, V. C.; Tomov, A.; Wass, D. F.; White, A. J. P.; Williams, D. J. *J. Chem. Soc., Dalton Trans.* **2002**, 2261−2262.

ethylene three times (5 min each) at rt, an appropriate amount of MAO was loaded and the reactor was immediately charged with ethylene to the desired pressure. The polymerization was allowed to run for the allotted time at the desired temperature and pressure. The reaction was stopped by the release of ethylene and the addition of 2-propanol and hexanes. PE was precipitated by the addition of MeOH containing a small amount of HCl. PE was then filtered and washed with water, methanol, acetone, and hexanes. The polymer was then dried in vacuo overnight.

General Procedure D: Ethylene Polymerization by Preactivated Pd^{II} Complexes 5 and 6. Approximately 10 μmol of catalyst was dissolved in 10 mL of toluene. Into a 600 mL Parr reactor purged under nitrogen, 55 mL of toluene solvent was loaded followed by purging with 50 psi ethylene three times (5 min each) at rt. After the catalyst solution was introduced at rt, the reactor was immediately charged with ethylene to the desired pressure. The polymerization was allowed to run for the allotted time. The desired temperature was reached within 5 min after the catalyst was loaded into the reactor. The reaction was stopped by the release of ethylene. Removal of solvent afforded PEs. To remove the catalyst residue, the crude products were dissolved in hexanes, decanted via pipet, and dried in vacuo for 1 h to afford clean PEs.

General Procedure E: In Situ Formation of Pd(Me)-Cl Complexes. After cooling a DCM solution of $(PhCN)_2PdCl_2$ (0.1 M) to −40 °C, tetramethyltin (3.0 equiv) was added. The mixture was stirred for 1 h at −40 °C, then warmed to −30 °C and allowed to stir for the allotted time period, resulting in the formation of a shiny silvery precipitate and a gray solution. An appropriate ligand dissolved in DCM (0.3 M) was added to the above solution at −30 °C. The resulting mixture was allowed to stir at −30 °C for 30 min before slowly warming to room temperature. The reaction was allowed to run for the allotted time period. Using a small Celite plug, the solution was filtered, concentrated, and precipitated with hexanes. The resulting complex was washed with ether followed by drying in vacuo overnight.

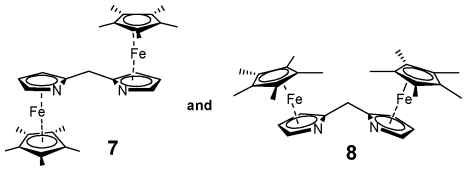

7 8

Bis(1′,2′, 3′, 4′, 5′-pentamethylazaferrocen-2-yl)methane (Cp*$_2$Fe$_2$DPM) (7 and 8). Following a literature procedure by Fu and co-workers,[36] di(2-pyrrole)methane (1.25 g, 8.55 mmol) was dissolved in 55 mL of THF. To the clear solution at rt was added 1.6 M *n*-BuLi (11.3 mL, 18.1 mmol), affording a light brown solution, and the mixture was allowed to stir for 15 min. The solution was transferred via cannula to AgCN (1.18 g, 8.82 mmol) slurry in THF (25 mL), and AgCN slowly dissolved in approximately 10 min to form a black solution (I).

To a solution of Cp*H (4.66 g, 34.2 mmol) in THF (210 mL) at rt was added 1.6 M *n*-BuLi (22.0 mL, 35.2 mmol). The resulting tan slurry was allowed to stir at rt for 15 min and transferred via cannula to a rapidly stirring $FeCl_2$ (4.54 g, 35.8 mmol) slurry in THF (140 mL) at −20 °C. The resulting lime green solution was stirred at −20 °C for 10 min. The black solution (I) was transferred via cannula to the $[Cp^*FeCl]_n$ solution, affording a brown solution. The resulting solution was allowed to react overnight (12 h). The reaction was quenched by addition of 2,2′-dipyridyl (3.44 g, 22.0 mmol) dissolved in MeOH (14 mL). The solution was passed through a silica plug and washed with EtOAc and hexanes. The solvent was removed, leaving a dark red oil that crystallized within a hour. Flash chromatography (under N_2) was carried out with the following gradient: 75:25:5 hexanes/EtOAc/Et_3N → 60:40:5 hexanes/EtOAc/Et_3N → 25:75:5 hexanes/EtOAc/Et_3N. Decamethylferrocene eluted first as a yellow band, followed by an orange-red band (±-(*S*,*S*)- and (*R*,*R*)-Cp*$_2$Fe$_2$DPM), a violet band, and finally an orange-red band (*meso*-Cp*$_2$Fe$_2$DPM). The solvent was then removed to obtain ±-(*S*,*S*)- and (*R*,*R*)-Cp*$_2$-Fe$_2$DPM (1.75 g, 38%, a dark red solid) and *meso*-Cp*$_2$Fe$_2$DPM (1.17 g, 26%, a dark red solid) for an overall yield of 65%.

^{1}H NMR of ±-(*S*,*S*)- and (*R*,*R*)-Cp*$_2$Fe$_2$DPM (500 MHz, C_6D_6): δ 1.89 (s, 30H), 3.73 (s, 2H), 3.87 (d, 2H, J = 1.5 Hz), 4.04 (s, 2H), 4.82 (s, 2H). LRMS (ES/MS, *m*/*z* in MeOH): Anal. Calcd for $Fe_2C_{29}H_{38}N_2$: 526.17 (M + H$^+$). Found: 526.17. ^{1}H NMR and MS spectra are consistent with the authentic sample as reported in Fu et al.[36]

^{1}H NMR of *meso*-Cp*$_2$Fe$_2$DPM (500 MHz, C_6D_6): δ 1.84 (s, 30H), 3.79 (s, 2H), 4.01 (s, 2H), 4.02 (d, 1H, J = 15.4 Hz), 4.09 (d, 1H, J = 15.4 Hz), 4.81 (s, 2H). LRMS (ES/MS, *m*/*z* in MeOH): Anal. Calcd for $Fe_2C_{29}H_{38}N_2$: 526.17 (M + H$^+$). Found: 526.17. ^{1}H NMR and MS spectra are consistent with the authentic sample as reported in Fu et al.[36]

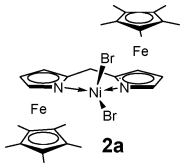

2a

±-(*S*,*S*)- and (*R*,*R*)-Cp*$_2$Fe$_2$DPM-Nickel(II) Bromide Complex (2a). In a 5 mL scintillation vial, ±-(*S*,*S*)- and (*R*,*R*)-Cp*$_2$Fe$_2$DPM (34.6 mg, 0.0658 mmol) were dissolved in 2 mL of DCM. To the red-orange solution, (DME)$NiBr_2$ (18.1 mg, 0.0586 mmol) was added and allowed to stir for 48 h. The brown solution was allowed to stir for 48 h, obtaining shiny brown crystals (33.8 mg, 52%). Combustion (C, H, N): Anal. Calcd for $NiFe_2C_{29}H_{38}N_2Br_2$: C, 46.77; H, 5.14; N, 3.76. Found: C, 44.22; H, 5.00; N, 3.54. Crystals suitable for X-ray crystal determination were grown by layering a chloroform solution of ±-(*S*,*S*)- and (*R*,*R*)-Cp*$_2$Fe$_2$DPM-nickel(II) bromide with hexanes.

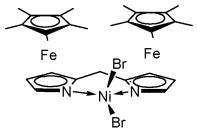

15

***meso*-Cp*$_2$Fe$_2$DPM-Nickel(II) Bromide Complex (15).** Following procedure A, *meso*-Cp*$_2$Fe$_2$DPM (87.0 mg, 0.165 mmol) was dissolved in 8 mL of DCM. To the red-orange solution was added (DME)$NiBr_2$ (43.7 mg, 0.142 mmol), and the mixture was allowed to stir for 48 h. A brown powdery solid was obtained (73.4 mg, 69%). Combustion (C, H, N): Anal. Calcd for $NiFe_2C_{29}H_{38}N_2Br_2$: C, 46.77; H, 5.14; N, 3.76. Found: C, 44.21; H, 5.07; N, 3.79.

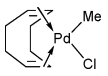

(Cycloocta-1,5-diene)chloromethylpalladium(II), (COD-)Pd(Me)Cl (17). In a 25 mL RBF, (COD)$PdCl_2$ (2.54 g, 8.88 mmol) was dissolved in 125 mL of DCM. To the resulting yellow solution, tetramethyltin (2.22 mg, 12.4 mmol) was added. The reaction was allowed to stir for 30 h, resulting in a gray solution with dark gray precipitate. The solution was filtered through Celite. The solvent was removed while the temperature of the flask was strictly maintained at 0 °C, and washed with diethyl ether (3 × 2 mL) to afford an off-white

solid (2.00 g, 85%). ^{1}H NMR (400 MHz, $CDCl_3$): δ 1.19 (s, 3H), 2.45−2.70 (m, 8H), 5.16 (m, 2H), 5.93 (m, 2H). ^{13}C NMR (100 MHz, $CDCl_3$): δ 12.87, 28.11, 31.51, 101.27, 124.33.

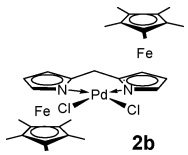

2b

±-(*S,S*)- and (*R,R*)-Cp*$_2$Fe$_2$DPM-Palladium(II) Chloride Complex (2b). Following procedure A, ±-(*S,S*)- and (*R,R*)-Cp*$_2$Fe$_2$DPM (49.0 mg, 0.0931 mmol) were dissolved in 2 mL of THF. To the red-orange solution was added (COD)-$PdCl_2$ (24.2 mg, 0.0848 mmol), and the mixture was allowed to stir for 2 days, resulting in the formation of an orange solution. An orange solid was obtained (45.9 mg, 70%). ^{1}H NMR (500 MHz, $CDCl_3$): δ 1.92 (s, 30H), 3.93 (s, 2H), 4.27 (s, 2H), 4.34 (s, 2H), 6.31 (s, 2H). ^{13}C NMR (125 MHz, $CDCl_3$): δ 11.34, 25.26, 74.64, 75.30, 83.57, 91.78, 95.43. Combustion (C, H, N): Anal. Calcd for $PdFe_2C_{29}H_{38}N_2Cl_2$: C, 49.51; H, 5.44; N, 3.98. Found: C, 50.25; H, 5.58; N, 4.17. HRMS (ES/MS, *m*/*z* in MeOH): Anal. Calcd for $PdFe_2C_{29}H_{38}N_2Cl + CH_3OH$: 699.0733 ($M - Cl^-$). Found: 699.0736.

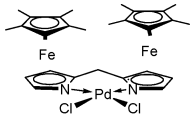

16

***meso*-Cp*$_2$Fe$_2$DPM-Palladium(II) Chloride Complex (16).** Following procedure A, *meso*-Cp*$_2$Fe$_2$DPM (47.9 mg, 0.0910 mmol) was dissolved in 8 mL of DCM. To the red-orange solution was added (COD)$PdCl_2$ (23.6 mg, 0.0827 mmol), affording an orange suspension. An orange powder was obtained (44.6 mg, 77%). ^{1}H NMR (500 MHz, $CDCl_3$): δ 2.05 (s, 30H), 3.55 (d, 1H, J = 14.5 Hz), 4.05 (s, 2H), 4.12 (s, 2H), 4.17 (d, 1H, J = 14.9 Hz), 5.74 (s, 2H). ^{13}C NMR (125 MHz, $CDCl_3$): δ 11.01, 26.74, 73.37, 74.72, 83.47, 91.76, 95.49. Combustion (C, H, N): Anal. Calcd for $PdFe_2C_{29}H_{38}N_2Cl_2$: C, 49.51; H, 5.44; N, 3.98. Found: C, 50.57; H, 5.74; N, 3.85. HRMS (ES/MS, *m*/*z* in MeOH): Anal. Calcd for $PdFe_2C_{29}H_{38}N_2Cl_2$: 667.0470 ($M - Cl^-$). Found: 667.0441.

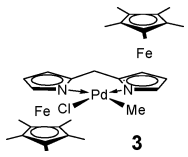

3

(*S,S*)- and (*R,R*)-Cp*$_2$Fe$_2$DPM-Palladium(methyl) Chloride(II) Complex (3). Following procedure A, ±-(*S,S*)- and (*R,R*)-Cp*$_2$Fe$_2$DPM (526 mg, 1.00 mmol) were dissolved in 16 mL of DCM. To the red-orange solution, (COD)Pd(Me)Cl (260 mg, 0.982 mmol) was added, and the mixture was allowed to stir for 36 h, resulting in the formation of a peach-colored suspension. After washing the solid with ether (3 × 3 mL) and drying in vacuo for 30 min, an off-peach solid was obtained (566 mg, 84%). The structure of **3** was fully assigned by various correlation NMR spectra (see Supporting Information). ^{1}H NMR (500 MHz, $CDCl_3$): δ 0.79 (s, 3H), 1.86 (s, 15H), 1.87 (s, 15H), 3.81 (d, 1H, J = 16.4 Hz), 3.87 (d, 1H, J = 16.4 Hz), 4.10 (s, 1H), 4.19 (s, 1H), 4.32 (d, 2H, J = 2.9 Hz), 5.33 (s, 1H), 5.89 (s, 1H). ^{13}C NMR (125 MHz, $CDCl_3$): δ −3.06 (Pd-*C*H$_3$), 10.99 (*cis*-Pd(Me)-C$_5$(*C*H$_3$)$_5$), 11.31 (*trans*-Pd(Me)-C$_5$(*C*H$_3$)$_5$), 26.06 (pyrr-*C*H$_2$-pyrr), 73.57 (*trans*-Pd(Me)-γ-pyrr-*C*H), 74.67 (*cis*-Pd(Me)-γ-pyrr-*C*H), 74.85 (*trans*-Pd(Me)-β-pyrr-*C*H), 75.61 (*cis*-Pd(Me)-β-pyrr-*C*H), 82.09 (*cis*-Pd(Me)-*C*$_5$(CH$_3$)$_5$), 82.56 (*trans*-Pd(Me)-*C*$_5$(CH$_3$)$_5$), 90.67 (*cis*-Pd(Me)-α-pyrr-*C*H), 91.13 (*trans*-Pd(Me)-α-pyrr-*C*H), 97.88 (*trans*-Pd(Me)-δ-pyrr-*C*), 99.15 (*cis*-Pd(Me)-δ-pyrr-*C*). Combustion (C, H, N): Anal. Calcd for $PdFe_2C_{30}H_{41}N_2Cl$: C, 52.74; H, 6.05; N, 4.18. Found: C, 52.05; H, 5.93; N, 4.10. HRMS (ES/MS, *m*/*z* in MeCN): Anal. Calcd for $PdFe_2C_{30}H_{41}N_2Cl$: 688.1285 ($M - Cl^- + MeCN$). Found: 688.1276.

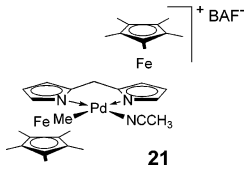

21

(*S,S*)- and (*R,R*)-Cp*$_2$Fe$_2$DPM-Pd(Me)NCCH$_3^+$BAF$^-$ (21). Following procedure B, ±-(*S,S*)- and (*R,R*)-Cp*$_2$Fe$_2$DPM-Pd-(Me)Cl (75.3 mg, 0.11 mmol) were suspended in 2 mL of DCM. To the red-orange suspension, NaBAF (97.5 mg, 0.11 mmol) was added followed by the addition of ACN (0.5 mL). The resulting solution was allowed to stir for 12 h. An orange-red crystalline solid was obtained (167.7 mg, 98%). The structure of **3** was fully assigned by various correlation NMR spectra (see Supporting Information). ^{1}H NMR (500 MHz, $CDCl_3$): δ 0.77 (s, 3H), 1.80 (s, 30H), 2.36 (s, 3H), 3.85 (d, 1H, J = 16.8 Hz), 3.89 (d, 1H, J = 16.7 Hz), 4.30 (s, 1H), 4.31 (s, 1H), 4.39 (d, 1H, J = 2.1 Hz), 4.42 (s, 1H), 4.87 (s, 1H), 5.20 (s, 1H), 7.61 (s, 4H), 7.79 (s, 8H). ^{13}C NMR (125 MHz, $CDCl_3$): δ 0.40 (Pd-*C*H$_3$), 3.24 (Pd-NC*C*H$_3$), 10.83 (*trans*-Pd(Me)-C$_5$(*C*H$_3$)$_5$), 10.99 (*cis*-Pd(Me)-C$_5$(*C*H$_3$)$_5$), 25.57 (pyrr-*C*H$_2$-pyrr), 74.50 (*cis*-Pd(Me)-γ-pyrr-*C*H), 75.70 (*trans*-Pd(Me)-β-pyrr-*C*H), 75.85 (*cis*-Pd(Me)-β-pyrr-*C*H), 76.22 (*trans*-Pd(Me)-γ-pyrr-*C*H), 82.67 (*trans*-Pd(Me)-*C*$_5$(CH$_3$)$_5$), 83.36 (*cis*-Pd(Me)-*C*$_5$(CH$_3$)$_5$), 89.74 (*cis*- and *trans*-Pd(Me)-α-pyrr-*C*H), 97.64 (*trans*-Pd(Me)-δ-pyrr-*C*), 98.29 (*cis*-Pd(Me)-δ-pyrr-*C*), 117.66 (*C*$_p$-BAF), 117.69 (*C*$_p$-BAF), 120.14 (Pd-N*C*CH$_3$), 124.81 (q, J_{CF3} = 272.9 Hz), 129.15 (q, J_{Cm} = 32.7 Hz), 135.04 (C$_o$-BAF), 161.96 (q, J_{B-C} = 50.3 Hz, C$_{ipso}$). Combustion (C, H, N): Anal. Calcd for $C_{64}H_{56}N_3BF_{24}Fe_2Pd$: C, 49.53; H, 3.64; N, 2.71. Found: C, 48.47; H, 3.58; N, 2.62. HRMS (ES/MS, *m*/*z* in DCM): Anal. Calcd for $C_{64}H_{56}N_3BF_{24}Fe_2Pd$: 688.1285 ($M^+ - BAF^-$). Found: 688.1299.

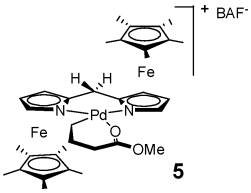

5

(*S,S*)- and (*R,R*)-Cp*$_2$Fe$_2$DPM-Pd(CH$_2$)$_3$COOMe$^+$BAF$^-$ (5). To the solution of DCM (2 mL) were added ±-(*S,S*)- and (*R,R*)-Cp*$_2$Fe$_2$DPM-Pd(Me)Cl (75.2 mg, 0.11 mmol). To the red-orange suspension was added methyl acrylate (10.9 μL, 0.121 mmol) followed by addition of NaBAF (97.5 mg, 0.11 mmol). The resulting deep red solution was allowed to stir for 12 h, filtered, and dried in vacuo overnight. An red-orange crystalline solid was obtained (175.7 mg, 90%). ^{1}H NMR (500 MHz, $CDCl_3$): δ 0.88 (d, 3H, J = 7.25 Hz), 0.90 (br s), 1.05 (m), 1.06 (br s), 1.33 (br s), 1.68−2.00 (m, 15H), 2.42 (s), 2.67 (br s, 2H), 3.3−3.4 (m, 1H), 3.7−4.6 (m, 9H), 4.9−5.2 (m, 1H), 7.61 (s, 4H, p-BAF-C*H*), 7.79 (o-BAF-C*H*). ^{13}C NMR (125 MHz, $CDCl_3$): δ 1.47, 11.02 (C$_5$*C*H$_3$), 11.27 (C$_5$*C*H$_3$), 22.20, 23.12, 23.48, 25.03, 25.47, 25.83, 35.85, 46.32, 55.18 (COO*C*H$_3^1$), 55.41 (COO*C*H$_3^2$), 74.54, 74.83, 75.60, 75.80, 75.89, 75.96, 76.21, 76.76, 82.78, 82.84, 83.51, 83.79, 88.42, 89.64, 89.79, 90.22, 97.11, 98.73, 99.32, 117.89 (*C*$_p$-BAF), 124.81 (q, J_{CF3} = 272.9 Hz), 128.67, 129.35 (q, J_{Cm} = 31.4 Hz), 135.26 (C$_o$-BAF), 161.77 (q, J_{B-C} = 50.3 Hz, C$_{ipso}$), 183.25 (*C*OOMe), 191.79 (*C*OOMe). Combustion (C, H, N): Anal. Calcd for $C_{66}H_{59}N_2O_2BF_{24}Fe_2Pd$: C, 49.64; H, 3.72; N, 1.75. Found: C, 49.02; H,

3.68; N, 1.83. HRMS (ES/MS, DCM, *m/z*): Anal. Calcd for $C_{66}H_{59}BF_{24}Fe_2N_2O_2Pd$: 733.1389 ($M^+ - BAF^-$). Found: 733.1381 (100%).

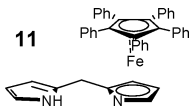

Cp°FeDPM-H (11). To Cp°H in THF (50 mL) was added 1.6 M ^{n}BuLi (2.8 mL, 4.5 mmol), affording an orange-yellow solution after stirring for 3 h at rt. The Cp°Li solution was added via cannula to the rapidly stirring $FeCl_2$ slurry, affording a purple solution that eventually changes to a transparent brown-green solution after 3 h of stirring at rt.

To DPM in THF (20 mL) was added 1.6 M ^{n}BuLi (2.2 mL, 3.50 mmol), affording a yellow solution. The resulting DPM−Li solution was allowed to stir for 15 min and was added via cannula to the brown-green Cp°FeCl solution, immediately forming an opaque brown solution. The brown solution was heated at 65 °C for 2 h and cooled to rt overnight, obtaining an off-red suspension. The reaction was quenched with MeOH (10 mL), passed through a 1 in. Celite plug, and washed with DCM to afford a red solution. The solvent was removed, providing a red solid. Flash chromatography (100:0 DCM/Et_3N → 100:1 → 100:5) afforded two bands: Cp°H (light yellow) and Cp°FeDPM-H (orange-red). A reddish-orange solid was obtained and dried in vacuo overnight (1.55 g, 69%). ^{1}H NMR (500 MHz, $CDCl_3$): δ 3.75 (d, 1H, J = 16.3 Hz), 3.81 (d, 1H, J = 16.3 Hz), 4.54 (d, 1H, J = 2.1 Hz), 4.58 (d, 1H, J = 1.6 Hz), 5.39 (s, 1H), 5.87 (s, 1H), 6.06 (m, 1H), 6.55 (m, 1H), 7.07−7.20 (m, 25H), 8.16 (br s, 1H). ^{13}C NMR (125 MHz, $CDCl_3$): δ 27.19, 76.41, 79.53, 88.17, 95.21, 106.29, 108.48, 108.85, 117.41, 127.02, 127.81, 129.39, 132.73, 135.13. Combustion (C, H, N): Anal. Calcd for $C_{44}H_{34}N_2Fe$: C, 81.73; H, 5.30; N, 4.33. Found: C, 80.00; H, 5.41; N, 4.20. HRMS (ES/MS, *m/z* in DCM): Anal. Calcd for $C_{44}H_{34}N_2Fe$: 647.2150 ($M + H^+$). Found: 647.2143 (100%).

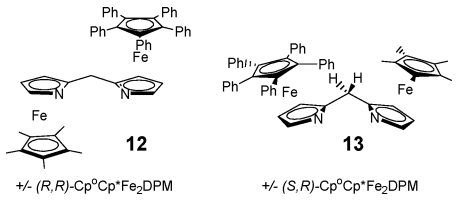

(1,2,3,4,5-Pentamethyl-1′,2′,3′,4′,5′-pentaphenylazaferrocen-2-yl)methane, (12 and 13). The monosubstituted complex Cp°FeDPM-H (204 mg, 0.316 mmol) was dissolved in 2.0 mL of THF. To the clear red solution at rt was added 1.6 M *n*-BuLi (0.22 mL, 0.35 mmol). The resulting deep red slurry was allowed to stir for 15 min (I).

To a solution of Cp*H (110 mg, 0.807 mmol) in THF (6.5 mL) at rt was added 1.6 M *n*-BuLi (0.55 mL, 0.88 mmol). The resulting tan slurry was allowed to stir at −20 °C for 15 min and transferred via cannula to a rapidly stirring $FeCl_2$ (109 mg, 0.858 mmol) slurry in THF (4.5 mL) at −20 °C. The [Cp*FeCl] solution stirred at −20 °C for 10 min. The deep red slurry (I) was transferred via cannula to the lime green $[Cp^*FeCl]_n$ solution. The brown solution was allowed to stir at rt for 15 h. The reaction was quenched by addition of 2,2′-dipyridyl (50 mg, 0.32 mmol) dissolved in MeOH (1 mL). The solution was passed through a Celite plug and washed with hexanes and EtOAc. The dark red solvent was removed, leaving a dark red solid. Flash chromatography (under N_2) was carried out with the following gradient: 20:80:1 hexanes/EtOAc/Et_3N → 40:60:1 hexanes/EtOAc/Et_3N → 60:40:1 hexanes/EtOAc/Et_3N. Decamethylferrocene eluted first as a yellow band, followed by an orange-red band for (*S*,*S*)- and (*R*,*R*)-Cp*Cp°Fe_2DPM and finally an orange-red band for (*S*,*R*)- and (*R*,*S*)-Cp*Cp°Fe_2DPM. The solvent was then removed to obtain (*S*,*S*)- and (*R*,*R*)-Cp*Cp°Fe_2DPM (114 mg, 43%, an orange-red solid) and (*S*,*R*)- and (*R*,*S*)-Cp*Cp°Fe_2DPM (113 mg, 43%, an orange-red solid) for an overall yield of 86%.

^{1}H NMR of (*S*,*S*)- and (*R*,*R*)-Cp*Cp°Fe_2DPM (500 MHz, $CDCl_3$): δ 1.82 (s, 15H), 3.70 (d, 1H, J = 14.5 Hz), 3.76 (d, 1H, J = 14.5 Hz), 3.99 (s, 2H), 4.48 (d, 1H, J = 1.9 Hz), 4.59 (d, 1H, J = 1.9 Hz), 4.79 (s, 1H), 5.30 (s, 1H), 7.10−7.15 (m, 10H), 7.16−7.22 (m, 15H). ^{13}C NMR (125 MHz, $CDCl_3$): δ 11.22, 29.45, 72.77, 75.95, 76.02, 79.83, 81.15, 88.16, 92.15, 94.76, 105.14, 109.43, 126.94, 127.77, 132.81, 135.26. Combustion (C, H, N): Anal. Calcd for $C_{54}H_{48}N_2Fe_2$: C, 77.52; H, 5.78; N, 3.35. Found: C, 76.11; H, 6.20; N, 3.44. HRMS (ES/MS, *m/z*): Anal. Calcd for $C_{54}H_{48}N_2Fe_2$: 837.2597 ($M + H^+$). Found: 837.2595 (100%).

^{1}H NMR of diastereomer: (*S*,*R*)- and (*R*,*S*)- Cp*Cp°Fe_2DPM (500 MHz, $CDCl_3$): δ 1.81 (s, 15H), 3.55 (d, 1H, J = 1.8 Hz), 3.60 (d, 1H, J = 15.5 Hz), 3.80 (d, 1H, J = 15.5 Hz), 4.01 (s, 1H), 4.32 (d, 1H, J = 1.8 Hz), 4.47 (d, 1H, J = 1.7 Hz), 4.87 (s, 1H), 5.32 (s, 1H), 7.0−7.12 (m, 10H), 7.14−7.19 (m, 15H). ^{13}C NMR (125 MHz, $CDCl_3$): δ 11.20, 28.55, 73.60, 75.22, 75.53, 79.12, 81.10, 88.06, 92.67, 95.28, 104.10, 109.69, 126.85, 127.73, 132.82, 135.38. Combustion (C, H, N): Anal. Calcd for $C_{54}H_{48}N_2Fe_2$: C, 77.52; H, 5.78; N, 3.35. Found: C, 75.75; H, 6.15; N, 3.37. HRMS (ES/MS, *m/z*): Anal. Calcd for $C_{54}H_{48}N_2Fe_2$: 837.2597 ($M + H^+$). Found: 837.2580.

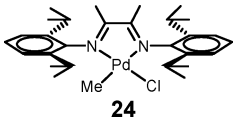

(Ar*N*=C(Me)−C(Me)C=*N*Ar)*Pd*(Me)Cl (Ar = 2,6-C6H3-(*i*-Pr)$_2$) (24). Using procedure E, $(PhCN)_2PdCl_2$ (203 mg, 0.528 mmol) was dissolved in DCM (5 mL). Tetramethyltin (0.22 mL, 1.62 mmol) was added and the mixture stirred for 2.5 h total (1.5 h at −30 °C). Bisimine ligand **23** (211 mg, 0.521 mmol) was dissolved in DCM (1.5 mL), affording an orange solution. The solution stirred for 5 h and filtered through Celite, and the solvent was removed. The orange solid was washed with ether (3 × 1 mL), affording the title compound **23** in 97% yield (285 mg). ^{1}H NMR of (Ar*N*=C(Me)−C(Me)C=*N*Ar)*Pd*(Me)Cl (Ar = 2,6-C6H3(*i*-Pr)$_2$) (400 MHz, $CDCl_3$): δ 0.53 (s, 3H), 1.18 (d, 6H, J = 2.1 Hz), 1.20 (d, 6H, J = 2.1 Hz), 1.36 (d, 6H, J = 6.8 Hz), 1.45 (d, 6H, J = 6.8 Hz), 2.04 (s, 3H), 2.07 (s, 3H), 3.06 (septet, 4H, J = 6.9 Hz), 7.24−7.32 (m, arom. 6H). The ^{1}H NMR spectra matched the authentic sample.[29]

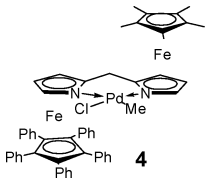

(*S*,*S*)- and (*R*,*R*)-Cp°Cp*Fe_2DPM-Palladium(methyl) Chloride(II) Complex (4). Following procedure E, $(PhCN)_2PdCl_2$ (181 mg, 0.472 mmol) was dissolved in DCM (4.8 mL). Tetramethyltin (0.21 mL, 1.54 mmol) was added and stirred for 2.0 h total (1 h at −30 °C). The unsymmetrical ligand (*S*,*S*)- and (*R*,*R*)-Cp°Cp*Fe_2DPM (306 mg, 0.365 mmol) dissolved in 3.0 mL of DCM was added to Pd(Me)Cl generated in situ (vide infra). The resulting red solution slowly warmed to rt (−30 °C → rt over 5 h). The solution was filtered through Celite, concentrated to ∼ 1 mL, and precipitated with hexanes. The peach solid was washed with ether (4 × 2 mL) and dried in vacuo for 30 min, affording the title Pd(Me)Cl complex as a peach solid (363 mg, 77%). The structure of **4** was fully assigned by various correlation NMR spectra, and the regiochemistry of the Pd-*Me* was established by nuclear Overhauser

effect (NOE) (see Supporting Information). ^{1}H NMR (500 MHz, $CDCl_3$): δ 0.92 (s, 3H), 1.83 (s, 15H), 3.40 (d, 1H, J = 2.1 Hz), 3.77 (s, 2H), 4.09 (s, 1H), 4.64 (s, 1H), 4.74 (s, 1H), 5.32 (s, 1H), 6.43 (s, 1H), 7.12 − 7.17 (m, 20H), 7.18−7.22 (m, 5H). ^{13}C NMR (125 MHz, $CDCl_3$): δ −2.19 (Pd-*C*H$_3$), 11.17 (*cis*-Pd-(Me)-C$_5$(*C*H$_3$)$_5$), 26.37 (pyrr-*C*H$_2$-pyrr), 75.37 (*cis*-Pd(Me)-γ-pyrr-*C*H), 76.36 (*cis*-Pd(Me)-β-pyrr-*C*H), 77.54 (*trans*-Pd(Me)-γ-pyrr-*C*H), 79.76 (*trans*-Pd(Me)-β-pyrr-*C*H), 82.65 (*cis*-Pd(Me)-*C*$_5$(CH$_3$)$_5$), 90.94 (*trans*-Pd(Me)-*C*$_5$(Ph)$_5$), 94.42 (*trans*-Pd(Me)-α-pyrr-*C*H), 97.40 (*cis*-Pd(Me)-δ-pyrr-*C*), 102.61 (*trans*-Pd(Me)-δ-pyrr-*C*), 127.01 (C$_p$), 127.16 (C$_p$), 127.81 (C$_o$), 128.00 (C$_o$), 132.73 (C$_p$), 132.95 (C$_p$), 134.23 (C$_5$-C$_{ipso}$), 135.14 (C$_5$-C$_{ipso}$). Combustion (C, H, N): Anal. Calcd for $C_{55}H_{51}N_2Fe_2PdCl$: C, 66.49; H, 5.17; N, 2.82. Found: C, 64.47; H, 5.31; N, 2.87. HRMS (ES/MS, *m*/*z* in CH_3CN/DCM (1:1 v/v)): Anal. Calcd for $C_{55}H_{51}N_2Fe_2PdCl$: 957.1809 (M − Cl). Found: 957.1827.

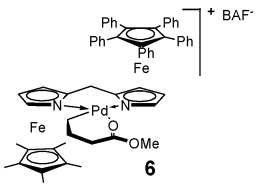

6

(*S*,*S*)- and (*R*,*R*)-Cp*Cp°Fe$_2$DPM-Pd(CH$_2$)$_3$COOMe$^+$BAF$^-$ (6). To the solution of DCM (2 mL) was added ±-(*S*,*S*)- and (*R*,*R*)-Cp°Cp*Fe$_2$DPM-Pd(Me)Cl (110 mg, 0.111 mmol). To the red-orange suspension was added methyl methacrylate (11.0 μL, 0.122 mmol) followed by addition of NaBAF (98.4 mg, 0.111 mmol). The resulting deep red solution was allowed to stir for 24 h, filtered, and dried in vacuo overnight. An orange-red crystalline solid was obtained (187.2 mg, 89%). ^{1}H NMR (500 MHz, $CDCl_3$): δ 0.66 (d, 3H, J = 7.28 Hz), 0.68 (br m), 0.95 (d, J = 7.09 Hz), 1.32 (br s), 1.55 (m), 1.65−1.76 (m, 15H), 1.83 (s), 1.91 (s), 1.95 (s), 2.01 (br m, 2H), 2.42 (s), 2.48 (m, 2H), 2.7 (m, 2H), 3.2 (m, 1H), 3.47 (s, 1H), 3.61 (s, 3H, O*Me*), 3.73 (s, 1H), 3.76 (s, 3H O*Me*^{1}), 3.82 (s, 1H), 3.85 (s, 1H), 4.05 (d, 1H, J = 2.43 Hz), 4.08 (d, 1H, J = 2.54 Hz), 4.13 (d, 1H, J = 6.21 Hz), 4.17 (d, 1H, J = 5.82 Hz), 4.33 (d, 1H, J = 1.40 Hz), 4.39 (d, 1H, J = 1.48 Hz), 4.95 (s, 1H), 4.99 (s, 1H), 5.02 (s, 1H), 5.05 (s, 2H), 5.57 (s, 1H), 5.65 (s, 1H), 5.9 (s, 1H), 7.00−7.30 (m, 25 H), 7.59 (s, 4H, p-BAF-C*H*), 7.78 (p-BAF-C*H*). ^{13}C NMR (125 MHz, $CDCl_3$): δ 1.24, 10.84 (C$_5$(*C*H$_3$)$_5$), 10.87 (C$_5$-(*C*H$_3$)$_5$), 15.49, 22.80, 23.21, 23.35, 25.30, 25.43, 25.50, 35.51, 45.82, 55.15 (COO*Me*), 55.24 (COO*Me*′), 66.06, 75.04, 75.44, 75.80, 76.22, 78.66, 79.52, 79.72, 79.83, 83.56, 83.70, 87.84, 88.44, 88.51, 89.13, 91.68, 92.68, 100.49, 117.66 (*C*$_p$-BAF), 124.79 (q, J_{CF3} = 271.5 Hz), 127.67, 127.73, 127.80, 129.12 (q, J_{Cm} = 31.4 Hz), 132.14, 132.32, 132.60, 133.09, 133.12, 135.03, 161.93 (q, J_{B-C} = 50.3 Hz, C$_{ipso}$), 182.92 (*C*OOMe), 191 (*C*OOMe). Combustion (C, H, N): Anal. Calcd for $C_{91}H_{69}BF_{24}Fe_2N_2O_2Pd$: C, 57.30; H, 3.65; N, 1.47. Found: C, 57.56; H, 3.63; N, 1.53. LRMS (ES/MS, DCM, *m*/*z*): Anal. Calcd for $C_{91}H_{69}BF_{24}Fe_2N_2O_2Pd$: 1043.22 (M$^+$ − BAF$^-$). Found: 1043.22 (100%).

X-ray Data Collection, Structure Solution, and Refinement for ±-(*S*,*S*)- and (*R*,*R*)-Cp*$_2$Fe$_2$DPM-Nickel (II) Bromide (2a). A maroon crystal of approximate dimensions 0.12 × 0.13 × 0.25 mm was mounted on a glass fiber and transferred to a Bruker CCD platform diffractometer. The SMART program package was used to determine the unit-cell parameters and for data collection (25 s/frame scan time for a sphere of diffraction data). The raw frame data were processed using SAINT[54] and SADABS[55] to yield the reflection data file. Subsequent calculations were carried out using the SHELXTL[56] program. The diffraction symmetry was *mmm*, and the systematic absences were consistent with the orthorhombic space group $P2_12_12_1$, which was later determined to be correct.

The structure was solved by direct methods and refined on *F* by full-matrix least-squares techniques. The analytical scattering factors[57] for neutral atoms were used throughout the analysis. Hydrogen atoms were included using a riding model. At convergence, wR2 = 0.1054 and Goof = 1.144 for 326 variables refined against 7226 data. As a comparison for refinement on *F*, R1 = 0.0441 for those 6392 data with $I > 2.0\sigma(I)$. The absolute structure could not be assigned by inversion of the model or by refinement of the Flack parameter.[58]

Low-Temperature NMR Kinetic Studies. Methyl Migratory Rate. An NMR tube with a screwcap was charged with 0.01 mmol of Pd(Me)Cl and 0.014 mmol of NaBAF in the glovebox. The NMR tube was wrapped with Teflon and capped followed by wrapping with electric tape. For the generation of the Pd(Me)(H_2C=CH_2) species, 1.0 equiv of ethylene (0.24 mL) was added at −78 °C, which is immediately followed by addition of CD_2Cl_2 (0.65 mL). The tube was shaken briefly for 15 min, and data points were collected at 30 min intervals to record the change in methyl peak at δ = 0.66 ppm with time at −14 °C.

Ethylene Consumption Rates. An NMR tube with a screwcap was charged with 0.01 mmol of Pd(Me)Cl and 0.014 mmol of NaBAF in the glovebox. The NMR tube was wrapped with Teflon and capped followed by wrapping with electric tape. For the generation of the Pd(Me)(H_2C=CH_2) species, 1 equiv of ethylene (0.24 mL) was added at −78 °C, which is immediately followed by addition of CD_2Cl_2 (0.65 mL). The tube was shaken briefly for 15 min, and excess ethylene (10 equiv, 2.4 mL volume) was added. Acquisition collection times were optimized at 6 s along with 7 scans to give an NMR spectrum. Data points were collected at 5−30 min intervals to record the change of free ethylene concentration with time at various temperatures.

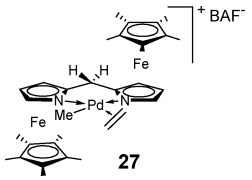

27

Generation of Cp*$_2$Fe$_2$DPM-Pd(Me)H$_2$C=CH$_2^+$BAF$^-$ (27). The complexes (*S*,*S*)- and (*R*,*R*)-Cp*$_2$Fe$_2$DPM-Pd(Me)Cl (**3**, 0.01 mmol, 1.0 equiv) and NaBAF (0.014 mmol, 1.4 equiv) were added to an NMR tube in the glovebox. The NMR tube was wrapped with Teflon and capped with a screwcap. The cap was further sealed with electric tape. The tube was cooled to −78 °C, and ethylene (0.24 mL, 1 equiv) was added, followed by addition of CD_2Cl_2 (0.65 mL). The methyl migratory insertion rate was followed by ^{1}H NMR overnight at 259.1 K. ^{1}H NMR (500 MHz, CD_2Cl_2, 259.1 K): δ 0.66 (s, 3H, Pd-*Me*), 1.68 (s, 15H), 1.84 (s, 15H), 3.82 (d, 1H, J = 16.8 Hz), 3.93 (d, 1H, J = 16.8 Hz), 4.27 (s, 1H), 4.37 (s, 1H), 4.57 (s, 1H), 4.65 (s, 1H), 4.69 (s, 1H), 4.70 (br s, 4H, *bound* H_2C=CH_2), 5.27 (s, 1H), 7.60 (s, 4H), 7.77 (s, 8H). Unbound ethylene appears at 5.43 ppm.

The rate data reported are based on one run with an automated integration of the peaks. The para-hydrogen of BAF (δ = 7.60 ppm) was used as an internal standard, and the following peaks were monitored for disappearance: δ = 5.43 (unbound ethylene) and 0.66 ppm (Pd-*Me*).

(54) *SMART Software Users Guide*, Version 5.1; Bruker Analytical X-Ray Systems, Inc.: Madison, WI, 1999.
(55) Sheldrick, G. M. *SADABS*, Version 2.03; Bruker Analytical X-Ray Systems, Inc.: Madison, WI, 2000.
(56) Sheldrick, G. M. *SHELXTL*, Version 5.10; Bruker Analytical X-Ray Systems, Inc.: Madison, WI, 1999.
(57) *International Tables for X-Ray Crystallography*; Kluwer Academic Publishers: Dordrecht, 1992; Vol. C.
(58) Flack, H. D. *Acta Crystallogr.* **1983**, *A39*, 876−881.

(1) First Methyl Migration. The first-order rate constant for the first olefin insertion was monitored by the disappearance of the Pd-*Me* group at 0.66 ppm over time. First methyl migratory insertion of ethylene by complex **27**: $k = 2.49 \times 10^{-5}$ s^{-1}, 259.1 K, $\Delta G^{\ddagger} = 20.6$ kcal/mol.

(2) Subsequent Olefin Insertions. The zero-order ethylene consumption rates were measured by monitoring the disappearance of the *unbound* ethylene at 5.43 ppm over time. The subsequent ethylene insertion by **27**: $k = 4.18 \times 10^{-5}$ s^{-1}, 255.7 K; $k = 1.08 \times 10^{-4}$ s^{-1}, 264.7 K, $\Delta G^{\ddagger} = 20.2$ kcal/mol; $k = 4.39 \times 10^{-4}$ s^{-1}, 273.7 K; $k = 4.18 \times 10^{-5}$ s^{-1}, 282.7 K; $k = 1.31 \times 10^{-3}$ s^{-1}. An Eyring plot of the rates at different temperatures gives $\Delta H^{\ddagger} = 18.2$ kcal/mol, $\Delta S^{\ddagger} = -7.4$ eu.

Acknowledgment. We thank the Petroleum Research Fund administered by the American Chemical Society, the National Science Foundation, the Army Research Office, and the University of California at Irvine for partial financial support. We thank Dr. Joseph Ziller for solving the X-ray crystal structure for complex **2a**, Dr. Phillip Dennison for help on NMR studies, Professors William J. Evans, Larry E. Overman, Scott D. Rychnovsky, Kenneth J. Shea, and Keith A. Woerpel for various help on lab instrumentation and chemicals, and the Evans group for helpful discussions on organometallic chemistry. Z.G. gratefully acknowledges an NSF CAREER Award, a Beckman Young Investigator Award, a DuPont Young Professor Award, and a 3M Non-Tenured Faculty Award.

Supporting Information Available: X-ray crystal structure data for complex **2a**, low-temperature NMR kinetic data, and NMR spectra (including correlation spectra) for characterization of various complexes and polymers. This material is available free of charge via the Internet at http://pubs.acs.org.

OM034051R